Kohn-Sham perturbation theory: Simple solution to variational instability of second order correlation energy functional

Hong Jiang[a] and Eberhard Engel
Center for Scientific Computing, JW Goethe-Universität Frankfurt, Max-von-Laue-Straße 1, D-60438 Frankfurt/Main, Germany

(Received 16 June 2006; accepted 28 September 2006; published online 13 November 2006)

The orbital-dependent correlation energy functional resulting from second order Kohn-Sham perturbation theory leads to atomic correlation potentials with correct shell structure and asymptotic behavior. The absolute magnitude of the exact correlation potential, however, is greatly overestimated. In addition, this functional is variationally instable, which shows up for systems with nearly degenerate highest occupied and lowest unoccupied levels like Be. In this contribution we examine the simplest resummation of the Kohn-Sham perturbation series which has the potential to resolve both the inaccuracy and the instability problem of the second order expression. This resummation includes only the hole-hole terms of the Epstein-Nesbet series of diagrams, which has the advantage that the resulting functional is computationally as efficient as the pure second order expression. The hole-hole Epstein-Nesbet functional is tested for a number of atoms and ions. It is found to reproduce correlation and ground state energies with an accuracy comparable to that of state-of-the-art generalized gradient approximations. The correlation potential, on the other hand, is dramatically improved compared to that obtained from generalized gradient approximations. The same applies to all quantities directly related to the potential, as, for instance, Kohn-Sham eigenvalues and excitation energies. Most importantly, however, the hole-hole Epstein-Nesbet functional turned out to be variationally stable for all neutral as well as all singly and doubly ionized atoms considered so far, including the case of Be. © *2006 American Institute of Physics*. [DOI: 10.1063/1.2370950]

I. INTRODUCTION

Kohn-Sham density functional theory[1–3] (KS-DFT) is currently undergoing a major transition. During the last decade it has become clear that the deficiencies of its present working horse, the generalized gradient approximation (GGA),[4] cannot be addressed by further refinement of this type of functional, which only depends on the local spin densities and their first and second gradients. This is true, in particular, for the incomplete cancellation of the self-interaction energy,[5] but also for the GGA's difficulties with long-range dispersion forces. The former problem is resolved in a systematic fashion by the use of the exact exchange of DFT, i.e., the Fock expression formulated in terms of the KS single-particle orbitals.[6,7] This functional extends the conventional GGA form in two directions. Being a functional of the KS orbitals, it incorporates much more detailed information on the electronic structure in an explicit form, similar to the KS kinetic energy. At the same time, it is fully nonlocal, i.e., the exact exchange energy density depends on the structure of the orbitals throughout all of space (and not just on their form in the immediate neighborhood of a single point). Still, the exact exchange is a proper density functional, as the KS orbitals are unique functionals of the ground state density. In view of the merits of this implicit density functional and its first-principles origin, the KS orbitals have been identified as the most promising set of basic variables for the next generation of exchange-correlation (xc) energy functionals E_{xc}.

Within this framework of orbital-dependent DFT it remains to find a suitable orbital-dependent representation of the correlation functional. In order to match the exact exchange this correlation functional should be fully nonlocal and have a first-principles background. Such functionals naturally emerge from the application of standard many-body methods as soon as the KS single-particle Hamiltonian $\hat{H}_s$ is used as noninteracting reference Hamiltonian.[8–13] In fact, the first order term resulting from a straightforward perturbation expansion with respect to the difference between the full Hamiltonian and $\hat{H}_s$ is nothing but the exact exchange of DFT. All higher order terms of the expansion thus constitute the correlation energy E_c.

The simplest correlation contribution, the second order term, consists of two components. The first, dominating component has the same functional form as the second order Møller-Plesset (MP2) energy, with the Hartree-Fock (HF) orbitals and eigenvalues replaced by their KS counterparts. The second term accounts for the difference between the reference Hamiltonians (KS versus HF) and turned out to be a minor correction.[10,11] We will therefore neglect this (negative definite) second component in the following and focus on the MP2-type expression E_c^{MP2}. This prototype first-principles correlation functional has been extensively studied for both atoms and molecules.[14–20] The results provide a mixture of

[a]Electronic mail: hong@th.physik.uni-frankfurt.de

promise and disappointment. On the one hand, E_c^{MP2} correctly accounts for the dispersion interaction[14,15] and the corresponding correlation potential v_c^{MP2} correctly reproduces the atomic shell structure and the asymptotic behavior of the exact atomic correlation potential.[19] On the other hand, both the energies and the potentials resulting from E_c^{MP2} significantly overestimate the corresponding exact reference data in those cases in which the latter are available for comparison.[10,19] What is more, E_c^{MP2} is found to be variationally instable for systems with a small gap between highest occupied molecular orbital–lowest unoccupied molecular orbital (HOMO-LUMO) gap[19,20] (as, for instance, the beryllium atom) and fails to describe chemical bonding in such elementary molecules as the nitrogen dimer.[11] It is obvious that the MP2 functional in its original form is not suitable as a universally applicable correlation functional for use with the exact exchange.

The failure of the MP2 functional emphasizes the importance of higher order correlation contributions. However, a "brute-force" inclusion of higher order terms, following the standard routes of wave-function-based quantum chemistry, is, while possible in principle, obviously not desirable within the framework of DFT. In view of the resulting computational cost such a DFT method would be restricted to the same limited range of applicability. One is thus led to search for less costly solutions to the instability and inaccuracy problem of E_c^{MP2}. One way to introduce higher order contributions in a numerically feasible way is to redefine the reference Hamiltonian used for the perturbation expansion, which is equivalent to summing up certain types of perturbation terms to infinite order. Following this line, Bartlett *et al.* obtained much improved results.[12,21]

In this work, an alternative, simple extension of the MP2 functional is put forward, which (i) resolves the problem of variational instability for many practical purposes, (ii) does not introduce additional computational cost, and (iii) turns out to correct the overestimation of correlation effects by the pure MP2 expression for all systems considered so far. Its form is inspired by the fact that the variational instability originates from the correlation-driven degeneracy of HOMO and LUMO KS levels, which lets the MP2 denominator shrink to zero.[19] This problem asks for the inclusion of a nonvanishing correction in the MP2 denominator, which reminds one of the Epstein-Nesbet (EN) expression for the correlation energy. Within DFT, EN-type corrections are obtained in a systematic fashion by a partial resummation of selected ladder-type Feynman diagrams of the KS perturbation series. The resulting shift in the MP2 denominator is negative definite if only hole-hole interactions are included, thus enlarging the absolute value of the MP2 eigenvalue denominator—even in the case of degenerate HOMO and LUMO states the hole-hole EN (HHEN) denominator remains nonzero. At the same time, all HHEN matrix elements are numerically available from the calculation of the exact exchange. Thus the most pragmatic and computationally cheapest way to cure the variational instability of the MP2 functional is to include exactly the HHEN corrections. Of course, it is not clear *a priori* whether this particular partial resummation also leads to a quantitative improvement over the MP2 approximation in those cases in which the latter can be applied. However, extensive tests for atoms and ions demonstrate that the HHEN expression represents clear progress also in this respect.

This paper is organized as follows. In the next section, the HHEN functional is introduced, followed by an explicit specification for spherical systems. In Sec. III, an extensive comparison of this functional with different conventional correlation functionals and its MP2 limit is reported. Section IV summarizes the results. Throughout this paper atomic units is used.

A preliminary report on part of this work, introducing the HHEN functional in an *ad hoc* fashion and presenting only few results, has been published in a recent conference proceedings volume.[22] In the present paper all details of the underlying theoretical formalism are given, including alternative resummations of the KS perturbation series. In addition, a much more extensive numerical investigation of the HHEN and related functionals is presented, in particular, addressing their variational properties.

II. THEORY

A. Kohn-Sham perturbation theory

Many-body theory on the basis of the KS system relies on the decomposition of the total Hamiltonian $\hat{H}$ into the KS Hamiltonian $\hat{H}_s$ and a perturbation,

$$\hat{H} = \hat{H}_s + \hat{H}_1, \tag{1}$$

$$\hat{H}_s = \hat{T} + \int d^3r \hat{n}(\boldsymbol{r}) v_s(\boldsymbol{r}), \tag{2}$$

$$\hat{H}_1 = \hat{W} + \int d^3r \hat{n}(\boldsymbol{r})[v_{\mathrm{ext}}(\boldsymbol{r}) - v_s(\boldsymbol{r})], \tag{3}$$

where $\hat{n}$ represents the density operator, v_s is the exact KS potential, v_{ext} abbreviates the external potential, and $\hat{W}$ denotes the electron-electron interaction. The KS potential consists of three contributions,

$$v_s(\boldsymbol{r}) = v_{\mathrm{ext}}(\boldsymbol{r}) + v_H(\boldsymbol{r}) + v_{\mathrm{xc}}(\boldsymbol{r}), \tag{4}$$

$$v_H(\boldsymbol{r}) = \int d^3r' \frac{n(\boldsymbol{r}')}{|\boldsymbol{r} - \boldsymbol{r}'|}, \tag{5}$$

$$v_{\mathrm{xc}}(\boldsymbol{r}) = \frac{\delta E_{\mathrm{xc}}[n]}{\delta n(\boldsymbol{r})}, \tag{6}$$

with n being the exact KS density,

$$n(\boldsymbol{r}) = \sum_i |\phi_i(\boldsymbol{r})|^2, \tag{7}$$

constructed from the KS single-particle orbitals,

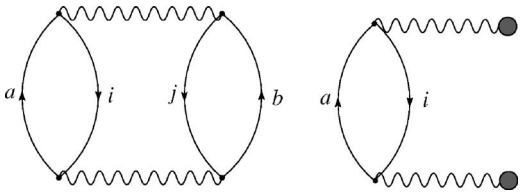

FIG. 1. Diagrammatic representation of second order correlation energy in KS-based perturbation theory. Brandow convention (Ref. 42) is used. Wiggly lines represent the antisymmetrized two-electron integrals (14); the external perturbation is defined in Fig. 2. Summation over a,b,i,j is implied.

$$\left\{-\frac{\nabla^2}{2}+v_s(\boldsymbol{r})\right\}\phi_p(\boldsymbol{r})=\varepsilon_p\phi_p(\boldsymbol{r}). \tag{8}$$

Throughout the paper $i,j,\ldots$ are used to denote occupied (hole) KS states, $a,b,\ldots$ for unoccupied (particle) states, and $p,q,\ldots$ for the general case.

Starting from (1), the exact xc energy can be expressed in terms of the KS single-particle orbitals and eigenenergies by application of the coupling-constant integration technique to the perturbation $\hat{H}_1$,[10,14]

$$E_{\mathrm{xc}}=E_x+\sum_{n=1}^{\infty}\frac{(-i)^n}{(n+1)!}\int_{-\infty}^{\infty}dt_1\cdots\int_{-\infty}^{\infty}dt_n \times\langle\Phi_0|T\hat{H}_{1,I}(0)\hat{H}_{1,I}(t_1)\cdots\hat{H}_{1,I}(t_n)|\Phi_0\rangle_l. \tag{9}$$

Here E_x is the exact exchange of DFT,

$$E_x=-\tfrac{1}{2}\sum_{ij}(ij||ji), \tag{10}$$

with $(ij\|ji)$ abbreviating the KS Slater integral,

$$(pq||rs)=\int d^3r\int d^3r'\frac{\phi_p^\dagger(\boldsymbol{r})\phi_r(\boldsymbol{r})\phi_q^\dagger(\boldsymbol{r}')\phi_s(\boldsymbol{r}')}{|\boldsymbol{r}-\boldsymbol{r}'|}. \tag{11}$$

$|\Phi_0\rangle$ is the ground state of the N-particle KS system,

$$\hat{H}_s|\Phi_0\rangle=\sum_i\varepsilon_i|\Phi_0\rangle, \tag{12}$$

$\hat{H}_{1,I}(t)$ represents $\hat{H}_1$ in the interaction picture with respect to $\hat{H}_s$, and the index l indicates that only linked diagrams have to be included in the evaluation of Eq. (9) via the Feynman diagram technique.

Equation (9) is most easily exploited by the application of straightforward perturbation theory.[10] To second order in $\hat{H}_1$ one ends up with the energy depicted in Fig. 1. The first of the diagrams in Fig. 1 directly translates into a MP2-type expression,

FIG. 2. Diagrammatic representation of Δ^{HF}, Eq. (15). The first term on the right hand side is the lowest order potential originating from the Coulomb interaction in $\hat{H}_1$, including the exchange term (Brandow convention is used). The second term represents the one-particle contribution in $\hat{H}_1$, i.e., $v_{\mathrm{ext}}(\boldsymbol{r})-v_s(\boldsymbol{r})$. The combination of these two terms serves as an effective one-body interaction, which vanishes in HF-based perturbation theory, but is finite in KS-based perturbation theory.

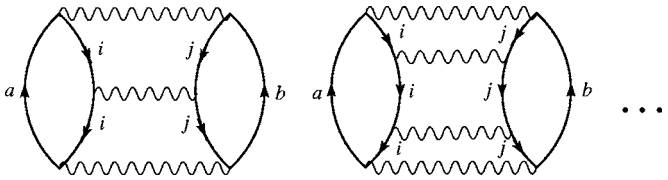

FIG. 3. Brandow diagram representation of the hole-hole Epstein-Nesbet perturbation series, E_c^{HHEN}, Eq. (18), in which only the diagonal elements of the hole-hole ladder diagrams are resummed to infinite order. Further inclusion of the corresponding particle-particle and hole-particle ladder diagrams leads to the full Epstein-Nesbet correlation energy E_c^{EN}, Eq. (19).

$$E_c^{\mathrm{MP2}}=\frac{1}{4}\sum_{ijab}\frac{|\langle ij||ab\rangle|^2}{\varepsilon_i+\varepsilon_j-\varepsilon_a-\varepsilon_b}, \tag{13}$$

where $\langle ij\|ab\rangle$ abbreviates the antisymmetrized two-electron integral,

$$\langle pq||rs\rangle:=(pq||rs)-(pq||sr). \tag{14}$$

The second diagram in Fig. 1 accounts for the fact that the present perturbation expansion is not based on the HF Hamiltonian, but rather on the KS Hamiltonian. In HF-based many-body perturbation theory the contributions of the single-particle operator in $\hat{H}_1$ are exactly canceled by a class of contractions of the two-particle operator in $\hat{H}_1$. The same is no longer true in Kohn-Sham perturbation theory (KSPT). Nevertheless, it is convenient to combine the appropriate contractions of $\hat{W}$ with the one-particle contribution and use the result as an effective one-particle operator (see Fig. 2). The matrix elements of this operator are given by

$$\Delta_{pq}^{\mathrm{HF}}=\sum_i\langle pi||qi\rangle+\langle p|v_{\mathrm{ext}}-v_s|q\rangle=\langle p|\hat{v}_x^{\mathrm{HF}}-v_{\mathrm{xc}}|q\rangle, \tag{15}$$

where

$$\langle p|\hat{v}_x^{\mathrm{HF}}|q\rangle=-\sum_i(pi||iq). \tag{16}$$

In view of Eq. (15) it is obvious that, as they stand, the two contributions to Fig. 1 are not yet fully consistent. While E_c^{MP2} is of second order in e^2, the right hand diagram contains higher order terms due to the dependence of $\Delta_{pq}^{\mathrm{HF}}$ on v_c. Thus, in order to be consistent in the order of e^2, these higher order terms have to be dropped, which leads to

$$E_c^{\Delta\mathrm{HF}}=\sum_{ia}\frac{|\langle i|\hat{v}_x^{\mathrm{HF}}-v_x|a\rangle|^2}{\varepsilon_i-\varepsilon_a}. \tag{17}$$

The results (13) and (17) agree with those obtained by an equivalent second order expansion of the adiabatic connection formula for E_c.[9]

The merits and deficiencies of E_c^{MP2} and $E_c^{\Delta\mathrm{HF}}$ have been extensively studied.[10,14,15,17–20] It was found that E_c^{MP2} is

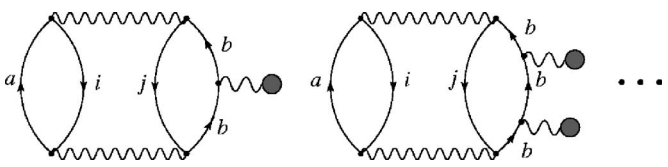

FIG. 4. Brandow diagrammatic representation of $E_c^{\mathrm{MP2}^*}$, Eq. (21).

TABLE I. Correlation energies (in mhartree) of closed-subshell atoms and ions. Results obtained from various xc functionals by insertion of the exact *x*-only KS orbitals and densities in comparison with exact data (Ref. 34). The last row provides the mean absolute percentage error (Δ) with respect to the exact energies.

Atom	Exact	VWN	LYP	PBE	MP2	HHEN	MP2*	EN	EN*
He	42	113	44	42	48	40	45	44	42
Li	45	152	53	51	49	44	46	46	44
Be	94	225	95	86	124	86	83	84	115
B^+	111	253	107	92	143	99	93	−18	138
C^{2+}	126	275	114	96	160	110	101	−63	157
N	188	429	192	180	216	186	191	243	200
O^+	194	462	207	189	215	190	194	239	204
F^{2+}	199	489	218	195	215	194	197	236	207
Ne	391	746	384	351	471	420	444	452	427
Na	396	805	408	372	459	419	428	443	415
Mg	438	892	459	411	514	458	454	448	461
Al^+	452	935	481	424	520	468	464	327	476
Si^{2+}	463	972	497	434	526	476	471	121	488
P	540	1118	566	526	623	561	557	743	575
S^+	556	1163	588	542	635	576	565	915	596
Cl^{2+}	570	1201	605	555	646	588	573	969	613
Ar	722	1431	751	707	849	767	778	849	776
Δ (%)		125	6	7	17	5	6	40	9

typically two orders of magnitudes larger than $E_c^{\Delta\mathrm{HF}}$. For that reason $E_c^{\Delta\mathrm{HF}}$ will be ignored in the following.

It has also become clear that higher order correlation contributions are required to resolve the most pressing deficiencies of E_c^{MP2}, its variational instability, and its drastic overestimation of correlation effects. However, in view of the origin of the instability, the correlation-driven breakdown of the HOMO-LUMO gap,[19] it is at least unclear whether a third order expansion (or any other finite order) will be sufficient to overcome this problem. In addition, the consistent inclusion of third order terms would substantially complicate corresponding KS calculations.

B. Partial resummation in KSPT

This suggests to resort to a (highly selective) partial resummation of the perturbation series. Ideally, this resummation should not introduce any additional computational effort, while ensuring a finite HOMO-LUMO gap. In standard many-body perturbation theory two types of resummations are known which comply at least with the first of these requirements.[24,25]

The first of these partial resummations is the EN series of ladder diagrams, illustrated in Fig. 3. If one restricts the resummation to the diagonal elements of the ladder diagrams, a simple MP2-type expression emerges, with an additional shift in the denominator. The result is particularly simple if only hole-hole contractions are included,

$$E_c^{\mathrm{HHEN}} = \frac{1}{4}\sum_{ijab} \frac{|\langle ij||ab\rangle|^2}{\varepsilon_i+\varepsilon_j-\varepsilon_a-\varepsilon_b-\langle ij||ij\rangle}. \tag{18}$$

E_c^{HHEN} will be called the hole-hole Epstein-Nesbet (HHEN) correlation functional in the following. The complete (second order) Epstein-Nesbet energy is obtained as soon as the corresponding particle-particle and particle-hole ladder diagrams are also taken into account,

$$E_c^{\mathrm{EN}} = \frac{1}{4}\sum_{ijab} \frac{|\langle ij||ab\rangle|^2}{\varepsilon_i+\varepsilon_j-\varepsilon_a-\varepsilon_b-\Delta_{ijab}^{\mathrm{EN}}}, \tag{19}$$

with

$$\Delta_{ijab}^{\mathrm{EN}} = \langle ij||ij\rangle + \langle ab||ab\rangle - \langle ia||ia\rangle - \langle jb||jb\rangle - \langle ib||ib\rangle - \langle ja||ja\rangle. \tag{20}$$

A second well-established resummation scheme addresses single-particle operators, as the effective potential (15). Resummation of the diagonal elements, as indicated in Fig. 4, results in a denominator shift $\Delta_{ii}^{\mathrm{HF}}+\Delta_{jj}^{\mathrm{HF}}-\Delta_{aa}^{\mathrm{HF}}-\Delta_{bb}^{\mathrm{HF}}$, so that the KS eigenenergies in the denominator of Eq. (13) are replaced by corresponding diagonal Fock-type matrix elements,

$$E_c^{\mathrm{MP2}^*} = \frac{1}{4}\sum_{ijab} \frac{|\langle ij||ab\rangle|^2}{f_{ii}+f_{jj}-f_{aa}-f_{bb}}, \tag{21}$$

$$f_{pq} \equiv \varepsilon_p\delta_{pq} + \Delta_{pq}^{\mathrm{HF}} = \langle p|-\frac{\nabla^2}{2}+v_{\mathrm{ext}}+v_H+\hat{v}_x^{\mathrm{HF}}|q\rangle. \tag{22}$$

Finally, one can combine both classes of diagrams allowing for the resummation to end up with[23,24]

$$E_c^{\mathrm{EN}^*} = \frac{1}{4}\sum_{i,j,a,b} \frac{|\langle ij||ab\rangle|^2}{f_{ii}+f_{jj}-f_{aa}-f_{bb}-\Delta_{ijab}^{\mathrm{EN}}}. \tag{23}$$

The occurrence of f_{pp} and/or $\langle pq||pq\rangle$ in Eqs. (19), (21), and (23) substantially complicates the application of these functionals, compared to that of E_c^{MP2}. On the one hand, the dependence on either f_{aa} or $\langle ab||ab\rangle$ drastically increases the number of matrix elements which have to be evaluated. On the other hand, even the dependence on f_{ii} represents a prob-

lem, as becomes clear as soon as the corresponding correlation potential is considered: v_c has to be calculated by the so-called optimized potential method (OPM),[25] whose basic ingredients are the functional derivatives of E_c with respect to ϕ_p and ε_p. These derivatives are rather easily evaluated for $\langle pq||pq\rangle$, but much more involved for f_{pp}, for which the functional derivatives of v_x with respect to ϕ_p and ε_p are required. While the technique for handling the latter problem is known,[9,11] its actual numerical realization is quite demanding. Consequently, only the simplest EN-type functional, Eq. (18), is as easily applied as E_c^{MP2}—the additional shift in the energy denominator of (18), $\langle ij||ij\rangle$, is evaluated anyway.

The motivation for considering the resummation schemes (18), (19), (21), and (23) solely comes from their practicability. However, the mere resummation of a particular class of diagrams does by no means imply that the resulting correlation energy represents an improvement over the pure MP2 term.[23,24] In fact, partial resummation can even lead to unphysical results, as explicitly demonstrated in Sec. III. The usefulness of a particular resummation thus needs to be verified by successful application to a wide variety of systems. In the present work this investigation is started by considering closed-subshell atoms.

C. Formulation for spherical systems

The expression (18) is very similar to the MP2 correlation energy, except for the state-dependent shift of the denominator. One can thus easily specialize the HHEN expression to the case of spherical systems, for which each KS orbital can be factorized as

$$\phi_p(\mathbf{r}) \equiv \frac{P_{nl\sigma}(r)}{r} Y_{lm}(\theta,\varphi)\chi_\sigma(s), \tag{24}$$

with n, l, m, and σ representing the principle, angular, magnetic, and spin quantum numbers, respectively, and Y_{lm} denoting a spherical harmonic. For spherical systems, the angular component of the orbitals can be treated analytically, so that the resulting energy is a functional of the radial wave functions only.

In the case of the EN-type energies, however, a technical difficulty arises. Due to the fact that the denominator shift $\langle ij||ij\rangle$ depends on the magnetic quantum numbers m_i and m_j, a straightforward analytical summation over m_i and m_j is no longer possible. This difficulty is closely related to a well-known deficiency of the EN expression. The EN correlation energy is not invariant under unitary transformation of degenerate orbitals.[24] In order to circumvent this problem, we use symmetry-averaged (SA) two-electron integrals in the denominator,

$$\langle ij||ij\rangle_{\mathrm{SA}} := \frac{1}{(2l_i+1)(2l_j+1)} \sum_{m_i,m_j} \langle ij||ij\rangle, \tag{25}$$

which is equivalent to restricting the basic EN expression to symmetry-adapted excitations. Using Wigner's $3j$ symbol, Eq. (25) reads explicitly

$$\langle ij||ij\rangle_{\mathrm{SA}} = R_0^{ijij} - \delta_{\sigma_i,\sigma_j} \sum_L \begin{pmatrix} l_i & L & l_j \\ 0 & 0 & 0 \end{pmatrix}^2 R_L^{ijji}. \tag{26}$$

Here R_L^{pqst} denotes the radial Slater integral,

$$R_L^{pqst} = \int_0^\infty dr \int_0^\infty dr' \frac{r_<^L}{r_>^{L+1}} P_p(r)P_q(r')P_s(r)P_t(r'), \tag{27}$$

with $r_< \equiv \min(r,r')$ and $r_> \equiv \max(r,r')$.

Using the symmetry-averaged denominator shift, the HHEN correlation energy for spherical systems, with spin taken into account explicitly, is given by

$$E_c^{\mathrm{HHEN}} = \frac{1}{2} \sum_{\sigma=\uparrow,\downarrow} \sum_{ijab\in\sigma} \sum_{L,L'} \frac{\delta_{L,L'} C_{D;L}^{ijab} (R_L^{ijab})^2 + C_{X;LL'}^{ijab} R_L^{ijab} R_{L'}^{ijba}}{\varepsilon_i+\varepsilon_j-\varepsilon_a-\varepsilon_b-\langle ij||ij\rangle_{\mathrm{SA}}} + \sum_{ia\in\uparrow,jb\in\downarrow} \frac{\sum_L C_{D;L}^{ijab} (R_L^{ijab})^2}{\varepsilon_i+\varepsilon_j-\varepsilon_a-\varepsilon_b-(ij||ij)_{\mathrm{SA}}}, \tag{28}$$

where the summation over $ijab$ has to be understood as a summation over the corresponding n and l quantum numbers. The coefficients $C_{D;LL'}^{ijab}$ and $C_{X;LL'}^{ijab}$ originate from the analytical summation of all m quantum numbers.[26] Their explicit forms are given in Ref. 19. Corresponding expressions are obtained for E_c^{EN}, $E_c^{\mathrm{MP2}^*}$, and $E_c^{\mathrm{EN}^*}$.

D. Numerical approach

In the case of orbital-dependent functionals the associated potential has to be calculated via the OPM.[25] The application of the OPM to MP2-type functionals turned out to be more intricate than in the case of the exact exchange,[16,18,27] the difficulties originating from the presence of continuum states in the MP2 functional. This problem can be resolved by employing a cavity approach,[19] in which hard-wall boundary conditions are imposed at a very large but finite radius around the atoms, thus suppressing true continuum states. As demonstrated in Ref. 19, this scheme does not only work in principle, but also provides a practical tool to apply the OPM to MP2-type functionals in a numerically exact way.

The cavity approach is also utilized in the present work. The reader is referred to Ref. 19 for all details. Here we restrict ourselves to summarizing the basic ingredients of the

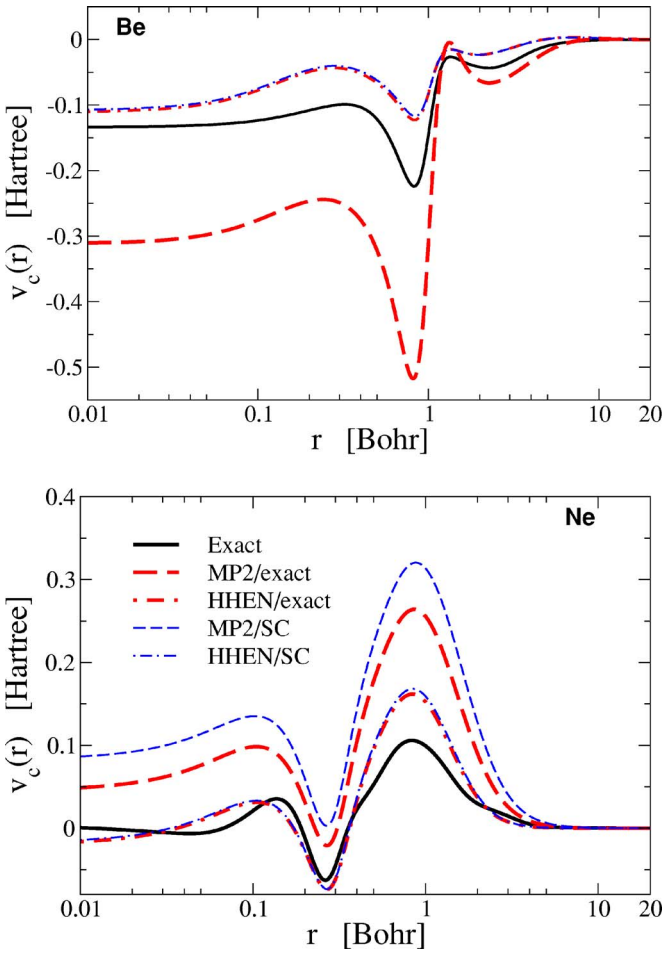

FIG. 5. (Color online) HHEN correlation potentials of Be and Ne vs v_c^{MP2}. Self-consistent results are compared to the potentials obtained from the exact KS densities for these atoms (Ref. 29). As reference, the exact correlation potential is also plotted.

approach. (1) The radial KS equations are solved via the Numerov method on a mixed logarithmic and linear grid, with hard-wall boundary conditions imposed at a large radius $R_{\max}$. (2) The kernel of the OPM equation, the static KS response function, is constructed in a numerically exact fashion by using the second, non-normalizable solution of the KS equation for a given eigenvalue. (3) The inhomogeneity of the OPM equation is consistently calculated by summation over all unoccupied states (wherever required). (4) The OPM equation on the radial grid is solved by a standard linear algebra solver. (5) The numerical output of this solver, which is contaminated by numerical noise in the semiasymptotic region and truncated at $R_{\max}$, is cleaned and extended to $r=\infty$ by fitting the appropriate asymptotic decay to the numerical solution.

The crucial parameters of this approach are the cavity radius $R_{\max}$ together with the number of shells $n_{\max}$ and maximum angular momentum $l_{\max}$ numerically included in sums over all unoccupied states. Quite generally, the number of shells required to achieve a given accuracy depends on the degree of localization of the occupied KS orbitals present in E_c^{MP2}. In all-electron calculations the degree of localization is determined by the $1s$ orbital. With increasing Z the $1s$ state becomes more and more localized, requiring a corresponding increase of $n_{\max}$. One finds empirically that the energy $\varepsilon_{\max}$ of the highest virtual shell required to achieve a fixed accuracy is linearly proportional to $|\varepsilon_{1s}|$, which essentially scales as the square of Z. For all atoms and ions considered in this paper $l_{\max}=6$ has been used. $R_{\max}$ and $n_{\max}$ have been chosen so that the relative error in the correlation energy is less than 1%.

III. RESULTS AND DISCUSSIONS

In order to establish the quality of the HHEN functional, we have carried out self-consistent calculations for a number of atoms, including all spherical (closed-shell or half-filled open shell) atoms or ions from He to Ar (referred to as H2A series in the following), the helium isoelectronic series from He to Ca^{18+} (He series), the neon isoelectronic series from Ne to Ni^{18+} (Ne series), and the argon isoelectronic series from Ar to Ni^{10+} (Ar series).[28] For all these atoms, highly accurate reference data for the ground state energy and ionization potential are available for comparison. In addition, the exact correlation potentials of He, Be, and Ne are known from accurate quantum Monte Carlo results,[29] allowing for a microscopic comparison between various approximate xc functionals.

As such two classes of functionals will be considered. The first-principles orbital-dependent E_c, i.e., Eqs. (13) (MP2), (21) ($\mathrm{MP2}^*$), (19) (EN), (23) (EN^*), and (18) (HHEN), will always be combined with the exact exchange (F). These combinations will be denoted as FMP2, etc. As a second class, three conventional xc functionals are included, i.e., the local density approximation (LDA),[30] BLYP (Refs. 31 and 32) ("best" semiempirical GGA functional), and PBE (Ref. 33) (best first-principles GGA).

A. Correlation energy

The performance of the partially resummed correlation functionals for the H2A series is shown in Table I. In order to allow for an unambiguous comparison, the densities and orbitals obtained from self-consistent calculations with only the exact exchange (referred to as x-only calculations in the following) have been used to evaluate the numbers of Table I. The resulting E_c are compared to exact quantum chemical correlation energies, obtained by combination of experimental ionization energies (corrected for relativistic and recoil effects) with highly accurate variational calculations for two- and three-electron systems.[34] While the quantum chemical E_c are not identical with the DFT correlation energies, the differences are quite small,[35] thus allowing the use of the quantum chemical values as reference data.

Table I demonstrates that the resummations E_c^{HHEN}, $E_c^{\mathrm{MP2}^*}$, and $E_c^{\mathrm{EN}^*}$ all three improve atomic correlation energies, as compared to the pure MP2 level. In fact, the average deviations obtained for these functionals are of the same size as those found for standard GGAs. On the other hand, E_c^{EN} shows drastic errors and even leads to unphysical positive correlation energies for B^+ and C^{2+}. The latter effect is due to the fact that the denominator shift in Eq. (19), $\Delta_{ijab}^{\mathrm{EN}}$, is not

TABLE II. Total ground state energies (in hartree) of closed-subshell atoms and ions obtained by self-consistent calculations with various xc functionals in comparison with exact data (Ref. 34). The last two rows show the mean and maximum absolute errors.

Atom	Exact	LDA	BLYP	PBE	FMP2	FHHEN
He	2.904	2.835	2.907	2.893	2.910	2.901
Li	7.478	7.344	7.483	7.462	7.482	7.476
Be	14.667	14.447	14.662	14.630	14.696[a]	14.659
B^+	24.349	24.038	24.337	24.293	24.380[a]	24.336
C^{2+}	36.535	36.130	36.514	36.461	36.568[a]	36.519
N	54.589	54.137	54.593	54.536	54.622	54.590
O^+	74.567	74.017	74.571	74.498	74.592	74.567
F^{2+}	97.808	97.158	97.812	97.725	97.829	97.807
Ne	128.938	128.233	128.973	128.866	129.027	128.970
Na	162.257	161.448	162.293	162.173	162.320	162.278
Mg	200.053	199.139	200.093	199.955	200.129	200.072
Al^+	242.126	241.101	242.168	242.013	242.194	242.141
Si^{2+}	288.458	287.318	288.501	288.330	288.521	288.470
P	341.259	340.006	341.278	341.116	341.340	341.278
S^+	397.729	396.357	397.749	397.569	397.806	397.746
Cl^{2+}	458.796	457.304	458.818	458.622	458.870	458.812
Ar	527.540	525.946	527.551	527.346	527.663	527.581
$\overline{\lvert\Delta\rvert}$		0.770	0.019	0.092	0.053	0.014
$\lvert\Delta\rvert_{\max}$		1.594	0.043	0.194	0.123	0.041

[a]From perturbative calculation based on the EXX density.

positive definite and can even change the sign of the complete denominator in extreme situations with nearly degenerate HOMO-LUMO levels.

As a result, E_c^{EN} is completely useless for the present purpose. E_c^{HHEN}, $E_c^{\mathrm{MP2}^*}$, and $E_c^{\mathrm{EN}^*}$, on the other hand, are comparable in accuracy, with E_c^{HHEN} being a little more accurate, so that the argument of computational efficiency clearly favors E_c^{HHEN}. The analysis of self-consistent results presented in the following sections is therefore restricted to E_c^{HHEN}.

B. Correlation potential and self-consistent stability

The main motivation for introducing the EN-type correction is to cure the variational instability of the MP2 expression, which manifests itself for the Be atom. The Be atom thus represents the natural starting point for an analysis of the variational stability of resummed functionals as HHEN. It turns out that self-consistency can be easily achieved with the HHEN expression. Figure 5(a) shows the resulting correlation potential in comparison with the exact v_c (Ref. 29) as well as with the v_c^{HHEN} and v_c^{MP2} obtained from the exact KS densities. Two observations are obvious: (i) the HHEN potential is much closer to the exact v_c than the perturbative result for v_c^{MP2}; (ii) the self-consistent v_c^{HHEN} is almost identical to the corresponding perturbative result, reflecting the stability of the HHEN potential with respect to changes of the KS orbitals. Both features are also observed for Ne, as shown in Fig. 5(b).

For all neutral, singly, and doubly ionized atoms considered so far the HHEN expression was found to be variationally stable. However, the HHEN resummation does not ensure variational stability under all circumstances. In the case of the Be isoelectronic series the breakdown reappears for Si^{10+}. The mechanism responsible is the same as observed for the MP2 functional in the case of neutral Be.[19] After a certain number of iterations the $2p$ eigenenergy dives into the occupied spectrum and finally becomes so much lower than the $2s$ eigenvalue that the eigenvalue difference dominates over the HHEN correction. For this mechanism to work, however, the $2s$-$2p$ gap must be rather small already without the inclusion of correlation. The relevant quantity is the ratio between the gap and the absolute values of the eigenenergies. This ratio shrinks with increasing Z, until for Si^{10+} it finally becomes sufficiently small, so that v_c can contract the $2p$ state so much that the gap breaks down.

Apparently, one would expect that this instability is also present for highly charged ions of the Mg-isoelectronic series. Extensive numerical calculations showed, however, that both the MP2 and the HHEN functionals are variationally stable for this isoelectronic series even for Z as high as 100 (Fm^{88+}). The difference between Be- and Mg-isoelectronic series can be traced to their different shell structures. Although in both cases one has an s-p HOMO-LUMO structure, the Mg series includes a p core state that has the same symmetry as the LUMO. This core state provides an additional "core repulsion" against the LUMO, preventing the radial contraction of the LUMO and the resulting energetic lowering.[36] This picture is confirmed by an investigation of the stability of the Ar-isoelectronic series. In this case the HOMO-LUMO structure is of $3p$-$3d$ type, so that the core repulsion effect is absent. Indeed one finds that for Fm^{82+} ($Z=100$) the MP2 functional is instable. The HHEN functional, one the other hand, remains stable even for this highly charged ion.

The near degeneracy of HOMO and LUMO levels for highly charged ions of the Be-isoelectronic series is well

known to represent a challenge for most single-determinant based many-body approaches, which is best demonstrated by the failure of conventional single-reference many-body perturbation theory and coupled-cluster methods to describe the dissociation of covalent bonds. In order to overcome these problems in the framework of DFT with orbital-dependent xc functionals, generalized KS perturbation theory based on either multireference KS states or ensembles is required. Nevertheless, the HHEN correction substantially extends the range of applicability of the MP2 expression, so that E_c^{HHEN} is an obvious candidate for resolving the instability problem for many practical purposes.

C. Self-consistent total ground state energies

Table II lists the total energies of the H2A series obtained by self-consistent calculations with different xc functionals. The results are compared to the corresponding exact data.[34] As reported in Ref. 19, the FMP2 functional gives ground state energies whose accuracy lies somewhere between the first-principles PBE-GGA and the semiempirical BLYP-GGA. The FHHEN functional significantly improves over the FMP2 approximation, so that the resulting total energies are slightly more accurate than the BLYP results.

In Fig. 6, the errors of ground state energies obtained with different xc functionals for the He, Ne, and Ar series are plotted as a function of Z. In all three cases, the PBE functional consistently underestimates the magnitude of ground state energies, with the error increasing almost linearly with Z. The BLYP functional is significantly more accurate than PBE. Nevertheless, it shows the same linear increase of the error with Z. As is well known, both the LDA and GGA are not able to describe the saturation of E_c with increasing nuclear charge.[37,38] In contrast, the FMP2 and FHHEN functionals systematically approach the exact E_c with increasing Z, the FHHEN results consistently being more accurate. As a result, the error in the total energy obtained from the FMP2 and FHHEN functionals decreases as a function of Z.

D. Ionization potential

As is well known, state-of-the-art GGA functionals give quite accurate ground state energies, but much less accurate xc potentials. In practice, the ionization potential (IP) is therefore usually calculated as total energy difference, rather than from the HOMO eigenvalue, to which, on the exact level, the IP is identical.[39] The difference between the exact IP and the HOMO eigenvalue therefore provides a simple quantitative measure of the quality of an approximate xc potential. Table III provides the IPs of the H2A series obtained with different xc functionals. The main outcome is that the combination of the exact exchange with MP2 correlation does not improve over the x-only results, while the FHHEN potential corrects more than 50% of the errors in the x-only IPs. This reflects the fact that the HHEN potential overestimates the amplitude of the outermost shell oscillation in the exact v_c much less than the MP2 potential (cf. Fig. 5).

The last column of Table III lists the HOMO energies resulting from the combination of the self-consistent x-only exchange potential with the v_c^{HHEN} obtained perturbatively from the exact x-only states. Little difference between the fully self-consistent HHEN results and these perturbative numbers is observed. Together with the accuracy of the corresponding perturbative correlation energies (see Table I) this suggests a perturbative handling of the HHEN functional on the basis of x-only calculations.

In Fig. 7 the percentage deviations of the HOMO eigenenergies of the He-, Ne-, and Ar-isoelectronic series are plotted as a function of Z. As in the H2A series, the IPs

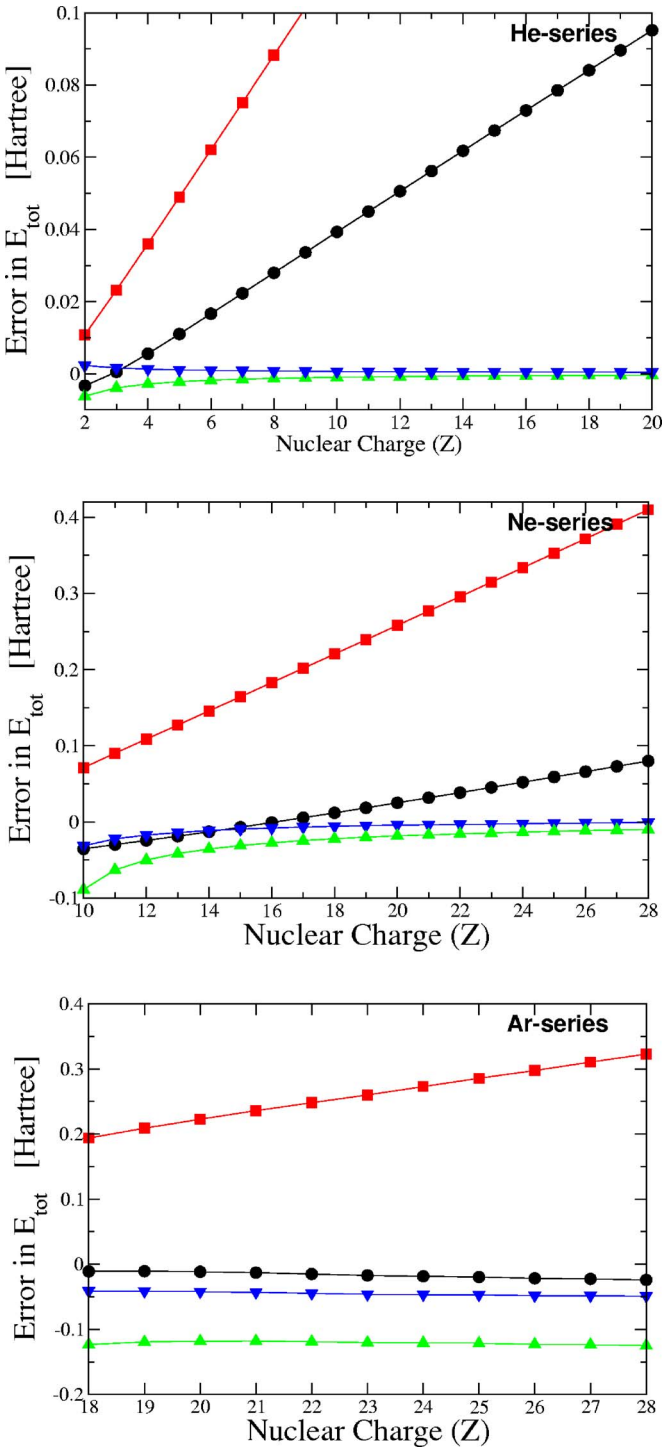

FIG. 6. (Color online) Errors in total ground state energies, $E_{\mathrm{tot}}^{(\mathrm{calc})}-E_{\mathrm{tot}}^{(\mathrm{exact})}$, obtained for the He-, Ne-, and Ar-isoelectronic series: FHHEN (triangle down) vs BLYP (circle), PBE (square), and FMP2 (triangle up) data.

TABLE III. HOMO eigenenergies (in hartree) of closed-subshell atoms and ions resulting from self-consistent calculations with different xc functionals in comparison with exact data (Ref. 34). The last two rows show the mean and maximum absolute errors.

							FHHEN	
Atom	Exact	x only	LDA	BLYP	PBE	FMP2	Self-consistent	Perturbation
He	0.904	0.918	0.570	0.585	0.579	0.893	0.913	0.914
Li	0.198	0.196	0.116	0.111	0.119	0.198	0.198	0.196
Be	0.342	0.309	0.206	0.201	0.206	0.368[a]	0.325	0.328
B^+	0.924	0.874	0.713	0.713	0.717	0.957[a]	0.898	0.901
C^{2+}	1.759	1.694	1.476	1.480	1.483	1.799[a]	1.726	1.729
N	0.535	0.571	0.309	0.297	0.307	0.503	0.534	0.535
O^+	1.292	1.331	0.972	0.962	0.971	1.273	1.295	1.297
F^{2+}	2.307	2.348	1.897	1.890	1.897	2.292	2.312	2.315
Ne	0.794	0.851	0.498	0.491	0.491	0.661	0.765	0.754
Na	0.189	0.182	0.113	0.106	0.113	0.191	0.189	0.188
Mg	0.281	0.253	0.175	0.168	0.173	0.298	0.275	0.277
Al^+	0.691	0.652	0.547	0.540	0.543	0.714	0.684	0.685
Si^{2+}	1.229	1.182	1.051	1.044	1.047	1.255	1.220	1.221
P	0.387	0.392	0.231	0.219	0.233	0.386	0.387	0.392
S^+	0.861	0.862	0.658	0.646	1.055	0.864	0.862	0.867
Cl^{2+}	1.459	1.459	1.214	1.204	1.218	1.466	1.462	1.466
Ar	0.582	0.591	0.382	0.373	0.378	0.562	0.578	0.583
$\overline{\lvert\Delta\rvert}$		0.028	0.212	0.218	0.212	0.024	0.009	0.010
$\lvert\Delta\rvert_{\max}$		0.065	0.410	0.417	0.410	0.134	0.034	0.040

[a]From perturbative calculation based on the EXX density.

calculated from the orbital-dependent functionals are much more accurate than the LDA or GGA results. In the limit of large Z the errors resulting from the FMP2 and FHHEN functionals vanish.

E. KS excitation energy

In order to examine the HHEN correlation potential further, KS excitation energies are studied, defined as the difference between the eigenvalues of occupied and unoccupied KS states. These eigenvalue differences can be regarded as the zeroth order contribution to the true excitation energies[40] and enter directly in time-dependent DFT calculations of excited states.[41]

Tables IV and V list the KS excitation energies of Be and Ne resulting from self-consistent calculations with different xc functionals. Only orbital-dependent functionals are considered at this point, since LDA and GGA potentials fail to reproduce the Rydberg states. One observes that (1) all functionals based on the exact exchange accurately reproduce the HOMO-LUMO gap, the error being one order of magnitude smaller than that found for other excitations; (2) inclusion of the HHEN correction into the MP2 expression leads to more accurate excitation energies than obtained by x-only calculations (which is not true for the pure MP2 potential).

Moreover, as in the case of the HOMO energy itself, the KS excitation energies resulting from perturbative inclusion of the HHEN potential (based on exact x-only orbitals) are again very close to the fully self-consistent results.

IV. CONCLUSIONS

In this paper, an orbital-dependent correlation functional based on the Epstein-Nesbet resummation of the perturbation series is introduced and applied to atomic systems. By retaining only the hole-hole contribution to the second order Epstein-Nesbet correlation energy, a functional (HHEN) is obtained whose structure is very close to that of the MP2 expression. The only difference is an additional sign-definite shift in the energy denominator, which promises an improved behavior in the case of nearly degenerate HOMO-LUMO states. As this shift is determined by Coulomb matrix elements of the occupied states only, the HHEN functional is computationally as efficient as its MP2 basis.

The HHEN functional has been tested extensively for a variety of atoms and ions. The main findings are the following. (1) When combined with the exact exchange, the HHEN functional gives correlation and total ground state energies with an accuracy comparable to that found for state-of-the-art GGAs. (2) The HHEN correlation potentials are much more accurate than those resulting from the pure MP2 approximation or from GGAs. In fact, the differences between the HHEN and the exact correlation potential are smaller than those between the exact v_c and zero (which is not the case for the MP2 approximation). (3) As a result, the HHEN potential undergoes only minor changes during self-consistent iteration—in contrast to the MP2 potential, which can even induce a variational breakdown in cases of near-degeneracy, like the Be atom. In fact, the HHEN functional turned out to be variationally stable for all neutral atoms as well as for all singly and doubly ionized ions considered up to now.

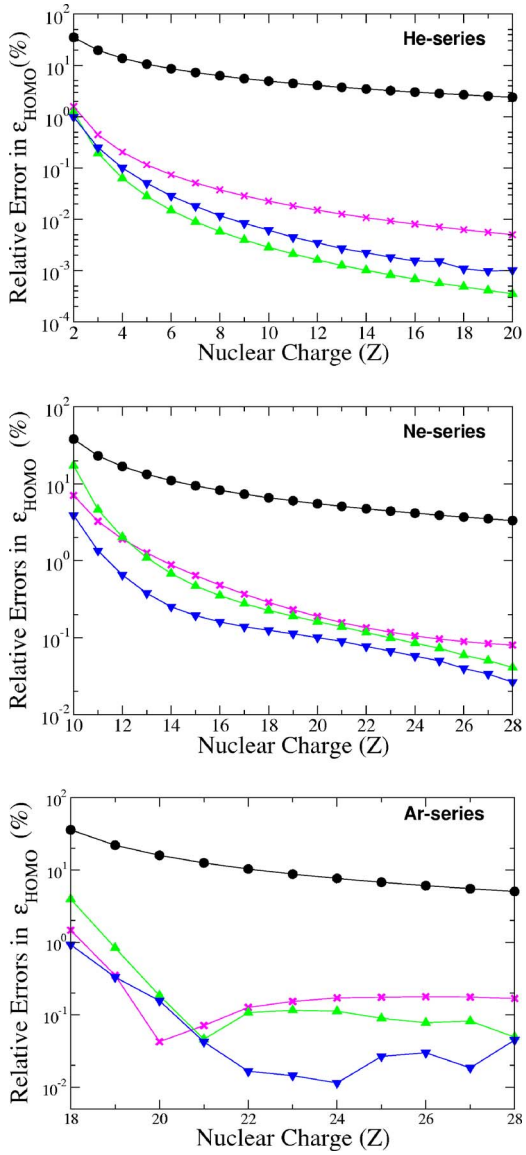

FIG. 7. (Color online) Absolute percentage errors of the HOMO eigenvalues of the He-, Ne-, and Ar-isoelectronic series with respect to "exact" values (Refs. 34 and 43): FHHEN (triangle down) vs *x* only (cross), BLYP (circles), and FMP2 (triangle up) data. Results from LDA and PBE are essentially identical to those of BLYP and are therefore not shown in the plot. In the Ar series, the error as a function of *Z* looks quite random, in contrast to that in He and Ne series, which is probably due to the numerical uncertainty in the estimated exact values(Ref. 34).

The insensitivity of the HHEN potential to the states used for its evaluation has important practical implications. Since the computational cost of the evaluation of the HHEN potential is much higher than that for calculating GGA potentials, the insensitivity suggests a perturbative implementation based on *x*-only solutions, which makes HHEN calculations feasible even for large molecular systems. The results of Sec. III demonstrate the accuracy of this perturbative approach.

The success of the HHEN functional for atomic systems makes it a promising candidate for a generally applicable correlation functional to be used in combination with the exact exchange. Its performance for molecules, however, remains to be investigated.

TABLE IV. KS excitation energies of the Be atom obtained from different xc functionals in comparison with exact data (Ref. 34). The last two rows show the mean and maximum absolute errors.

Excitation	Exact	*x* only	FHHEN	FHHEN(p)
$2s\rightarrow 2p$	0.133	0.131	0.133	0.133
$2s\rightarrow 3s$	0.244	0.217	0.232	0.235
$2s\rightarrow 3p$	0.269	0.241	0.256	0.259
$2s\rightarrow 3d$	0.283	0.253	0.269	0.272
$2s\rightarrow 4s$	0.296	0.264	0.279	0.282
$2s\rightarrow 4p$	0.305	0.273	0.287	0.291
$2s\rightarrow 4d$	0.310	0.278	0.292	0.296
$2s\rightarrow 5s$	0.315	0.283	0.297	0.300
$2s\rightarrow 5p$	0.319	0.287	0.301	0.304
$2s\rightarrow 6s$	0.325	0.292	0.306	0.309
$2s\rightarrow 6p$	0.327	0.294	0.308	0.312
$\overline{\lvert\Delta\rvert}$		0.029	0.015	0.012
$\lvert\Delta\rvert_{max}$		0.033	0.019	0.015

Moreover, the self-consistent implementation of the HHEN functional fails for the highly charged ions of the Be-isoelectronic series beyond Al^{9+}, due to a reordering of the HOMO and LUMO levels in the course of the self-consistent iteration. One would expect similar difficulties for molecular systems with nearly degenerate HOMO-LUMO states. In quantum chemistry, a sound description of such systems usually requires multireference techniques. There can be little doubt that analogous developments are necessary for a completely general formulation of orbital-dependent exchange-correlation functionals within DFT.

TABLE V. KS excitation energies of the Ne atom obtained from different xc functionals in comparison with exact data (Ref. 34). The last two rows show the mean and maximum absolute errors.

Excitation	Exact	*x* only	FHHEN	FHHEN(p)
$2s\rightarrow 3s$	1.469	1.526	1.432	1.428
$2s\rightarrow 3p$	1.542	1.604	1.504	1.502
$2s\rightarrow 3d$	1.595	1.661	1.558	1.555
$2s\rightarrow 4s$	1.582	1.646	1.545	1.542
$2s\rightarrow 4p$	1.602	1.667	1.564	1.562
$2s\rightarrow 4d$	1.620	1.686	1.583	1.580
$2s\rightarrow 4s$	1.615	1.681	1.578	1.575
$2s\rightarrow 5p$	1.623	1.689	1.586	1.583
$2s\rightarrow 6s$	1.629	1.695	1.592	1.589
$2s\rightarrow 6p$	1.633	1.699	1.596	1.593
$2p\rightarrow 3s$	0.612	0.659	0.580	0.577
$2p\rightarrow 3p$	0.684	0.736	0.653	0.650
$2p\rightarrow 3d$	0.738	0.793	0.707	0.704
$2p\rightarrow 4s$	0.725	0.779	0.694	0.691
$2p\rightarrow 4p$	0.744	0.799	0.713	0.711
$2p\rightarrow 4d$	0.763	0.819	0.732	0.729
$2p\rightarrow 5s$	0.758	0.813	0.727	0.724
$2p\rightarrow 5p$	0.766	0.821	0.735	0.732
$2p\rightarrow 6s$	0.772	0.828	0.741	0.738
$2p\rightarrow 6p$	0.776	0.832	0.745	0.742
$\overline{\lvert\Delta\rvert}$		0.059	0.034	0.037
$\lvert\Delta\rvert_{max}$		0.066	0.037	0.041

ACKNOWLEDGMENTS

Financial support by the Deutsche Forschungsgemeinschaft (Grant No. EN 265/4-2) is gratefully acknowledged. The calculations for this work have been performed on the computer cluster of the Center for Scientific Computing of JW Goethe-Universität Frankfurt.

[1] R. G. Parr and W. Yang, *Density-Functional Theory of Atoms and Molecules* (Oxford University Press, New York, 1989).
[2] R. M. Dreizler and E. K. U. Gross, *Density Functional Theory: An Approach to the Quantum Many-Body Problem* (Springer-Verlag, Berlin, 1990).
[3] *A Primer in Density Functional Theory*, edited by C. Fiolhais, M. Marques, and F. Nogeira (Springer, Berlin, 2003).
[4] J. P. Perdew and S. Kurth, in *A Primer in Density Functional Theory*, edited by C. Fiohais, F. Nogueira, and M. Marques (Springer, Berlin, 2003), Chap. 1, pp. 1–55.
[5] E. Engel and S. H. Vosko, Phys. Rev. B **47**, 13164 (1993).
[6] V. Sahni, J. Gruenebaum, and J. P. Perdew, Phys. Rev. B **26**, 4371 (1982).
[7] D. C. Langreth and M. J. Mehl, Phys. Rev. B **28**, 1809 (1983).
[8] L. J. Sham, Phys. Rev. B **32**, 3876 (1985).
[9] A. Görling and M. Levy, Phys. Rev. A **50**, 196 (1994).
[10] E. Engel and R. M. Dreizler, J. Comput. Chem. **20**, 31 (1999).
[11] E. Engel, in *A Primer in Density Functional Theory*, edited by C. Fiohais, F. Nogueira, and M. Marques (Springer, Berlin, 2003), Chap. 2, pp. 56–143.
[12] R. J. Bartlett, V. F. Lotrich, and I. V. Schweigert, J. Chem. Phys. **123**, 062205 (2005).
[13] A. Görling, J. Chem. Phys. **123**, 062203 (2005).
[14] E. Engel, A. F. Bonetti, S. Keller, I. Andrejkovics, and R. M. Dreizler, Phys. Rev. A **58**, 964 (1998).
[15] E. Engel, A. Höck, and R. M. Dreizler, Phys. Rev. A **61**, 032502 (2000).
[16] A. Facco Bonetti, E. Engel, R. N. Schmid, and R. M. Dreizler, Phys. Rev. Lett. **86**, 2241 (2001).
[17] I. Grabowski, S. Hirata, S. Ivanov, and R. J. Bartlett, J. Chem. Phys. **116**, 4415 (2002).
[18] E. Engel, H. Jiang, and A. Facco Bonetti, Phys. Rev. A **72**, 052503 (2005).
[19] H. Jiang and E. Engel, J. Chem. Phys. **123**, 224102 (2005).
[20] P. Mori-Sanchez, Q. Wu, and W. Yang, J. Chem. Phys. **123**, 062204 (2005).
[21] R. J. Bartlett, I. Grabowski, S. Hirata, and S. Ivanov, J. Chem. Phys. **123**, 062205 (2005).
[22] E. Engel and H. Jiang, Int. J. Quantum Chem. **106**, 3242 (2006).
[23] S. Wilson, *Electron Correlation in Molecules* (Clarendon, Oxford, 1984).
[24] A. Szabo and N. S. Ostlund, *Modern Quantum Chemistry* (McGraw-Hill, New York, 1989).
[25] J. D. Talman and W. F. Shadwick, Phys. Rev. A **14**, 36 (1976).
[26] M. E. Rose, *Angular Momentum in Quantum Mechanics* (Princeton University Press, Princeton, NJ, 1957).
[27] A. Facco Bonetti, E. Engel, R. N. Schmid, and R. M. Dreizler, Phys. Rev. Lett. **90**, 219302 (2003).
[28] For the H2A series, we use $R_{\max}(Z)=20.0$ bohr and $n_{\max}=400$. In the case of highly charged ions one can speed up the calculations by utilizing the fact that their effective size is determined by the r-expectation values of the most weakly bound orbitals. For isoelectronic series this r expectation is inversely proportional to Z, which allows to set the cavity radius as $R_{\max}(Z)=R_0N/Z$ (where N is the electron number of the ions). $R_0=10$ bohr and $n_{\max}=100$ have been used for the He series, and $R_0=20$ bohr and $n_{\max}=400$ for the Ne and Ar series.
[29] C. J. Umrigar and X. Gonze, Phys. Rev. A **50**, 3827 (1994).
[30] S. H. Vosko, L. Wilk, and M. Nusair, Can. J. Phys. **58**, 100 (1980).
[31] A. D. Becke, Phys. Rev. A **38**, 3098 (1988).
[32] C. Lee, W. Yang, and R. G. Parr, Phys. Rev. B **37**, 785 (1988).
[33] J. P. Perdew, K. Burke, and M. Ernzerhof, Phys. Rev. Lett. **77**, 3865 (1997).
[34] S. J. Chakravorty, S. R. Gwaltney, E. R. Davidson, F. A. Parpia, and C. Froese Fischer, Phys. Rev. A **47**, 3649 (1993).
[35] E. K. U. Gross, M. Petersilka, and T. Grabo, ACS Symp. Ser. **629**, 42 (1996).
[36] The underlying mechanism for the core repulsion effect is simple. For atomic orbitals with different angular symmetry, the orthogonality of the wave functions is ensured by their angular part. On the other hand, for orbitals with the same angular symmetry the radial orbitals have to be orthogonal to each other.
[37] A. A. Jarzecki and E. R. Davidson, Phys. Rev. A **58**, 1902 (1998).
[38] V. N. Staroverov, G. E. Scuseria, J. P. Perdew, J. Tao, and E. R. Davidson, Phys. Rev. A **70**, 012502 (2004).
[39] C.-O. Almbladh and U. von Barth, Phys. Rev. B **31**, 3231 (1985).
[40] A. Görling, Phys. Rev. B **53**, 7024 (1996).
[41] E. K. U. Gross, J. F. Dobson, and M. Petersilka, Top. Curr. Chem. **181**, 81 (1996).
[42] B. H. Brandow, Rev. Mod. Phys. **39**, 771 (1967).
[43] E. R. Davidson, S. A. Hagstrom, S. J. Chakravorty, V. Meiser Umar, and C. Froese Fischer, Phys. Rev. A **44**, 7071 (1991).